The Astrophysical Journal, 955:80 (12pp), 2023 September 20 https://doi.org/10.3847/1538-4357/ace905

KIC 9845907: A δ Scuti Star with the First Overtone as the Dominant Frequency and with Many Equidistant Structures in Its Spectrum

Xiao-Ya Sun[1], Zhao-Yu Zuo[1], Tao-Zhi Yang[1], and Antonio García Hernández[2]
[1] Ministry of Education Key Laboratory for Nonequilibrium Synthesis and Modulation of Condensed Matter, School of Physics, Xi'an Jiaotong University, Xi'an 710049, People's Republic of China; zuozyu@xjtu.edu.cn
[2] Departamento de Física Teórica y del Cosmos, Universidad de Granada, Campus de Fuentenueva s/n, E-18071, Granada, Spain
Received 2022 September 27; revised 2023 July 18; accepted 2023 July 18; published 2023 September 20

Abstract

In this paper, we present an analysis of the pulsating behavior of Kepler target KIC 9845907. Using the data from Kepler, we detected 85 significant frequencies, including the first overtone $f_1 = 17.597$ day^{-1} as the dominant frequency, the non-radial independent frequency $f_3 = 31.428$ day^{-1} ($\ell = 1$), as well as two modulation terms $f_{m1} = 0.065$ day^{-1} and $f_{m2} = 1.693$ day^{-1}. We found fourteen pairs of triplet structures with f_{m1} or f_{m2}, four pairs of which can further form quintuplet structures. We note these are the most intriguing features discovered in this study and they were recognized for the first time in δ Scuti stars. We discussed several possible explanations, i.e., beating, the Blazhko effect, combination mode hypothesis, nonlinear mode coupling, large separation, and stellar rotational splitting for these equidistant structures. Our asteroseismic models indicate this modulation with f_{m1} might be related to the rotational splitting. The study of more δ Scuti stars with triplet and/or quintuplet structures using high-precision space photometry would be helpful to further explore its origin.

Unified Astronomy Thesaurus concepts: Delta Scuti variable stars (370); Stellar oscillations (1617)

1. Introduction

One of the long-standing goals in astronomy is to improve our understanding of stellar internal structure and evolution. Asteroseismology, by comparing observations with theoretical models, constrains the interior physics of stars, such as convection, rotation, etc. (Aerts 2021). In recent years, asteroseismology has entered its golden age thanks to the continuous, long-term and high-resolution data from space telescopes such as Kepler (Koch et al. 2010) and Transiting Exoplanet Survey Satellite (TESS; Ricker et al. 2015). Significant progress has been made in the study of various types of pulsators, such as red giant stars (Yu et al. 2020; Li et al. 2022), solar-type stars (Chaplin & Miglio 2013), pulsating white dwarfs (Zong et al. 2016), and δ Scuti stars (Chen & Li 2019; Yang et al. 2022) as well. Among the more than 150,000 observed targets in the Kepler field, over 2000 δ Scuti stars have been discovered (Balona 2014; Bowman et al. 2016), which provides a large number of samples for asteroseismic studies.

δ Scuti stars are a class of short-period variables with periods in range of 0.02–0.25 days. They are intermediate-mass stars and have spectral types from A to F (Breger 2000). Their masses are generally between 1.5 $M_\odot$ and 2.5 $M_\odot$, which place them in the transition region between the lower-mass stars with thick convective envelope and radiative core and the massive ones with thin or none convective shell but a convective core (Aerts et al. 2010). They are located in the classical Cepheid instability strip where it crosses the main sequence (MS) in the Hertzsprung–Russell (H-R) diagram. Most δ Scuti stars are on the MS or post-MS stages although there are also some on the pre-MS stage (Breger 2000; Zwintz 2008). These variables exhibit both radial and non-radial modes (Qian et al. 2018; Sun et al. 2021), excited mainly by the κ mechanism (Aerts et al. 2010), usually identified as low-radial-order (n) low-angular-degree (l) pressure (p) modes (Uytterhoeven et al. 2011; Holdsworth et al. 2014). Moreover, Uytterhoeven et al. (2011) discovered that many of the δ Scuti stars show also gravity(g) modes. These characteristics make them excellent targets for asteroseismology study.

The pulsation spectra of δ Scuti stars are generally very rich and messy, which challenges the mode identification (Goupil et al. 2005; Bedding et al. 2023). Recently, there have been many studies on complex spectra from different perspectives, such as the low-order large separation (Rodríguez-Martín et al. 2020), rotational splitting (Ramón-Ballesta et al. 2021), (near-) equidistant frequency spacing structures (such as triplets and/or quintuplets; Kolenberg et al. 2011), and the relation between the low-order large separation and the stellar mean density (Suárez et al. 2014; García Hernández et al. 2015). For instance, in KIC 5950759, two pairs of triplet structures centered on the dominant frequency were detected in its frequency spectra, and the cause of that is inferred to be the amplitude modulation of stellar rotation (Yang et al. 2018). Another δ Scuti star KIC 10284901 shows two pairs of quintuplet structures, which might be related to the Blazhko effect (Yang & Esamdin 2019). Moreover, Chen et al. (2017) analyzed the frequency spectrum of CoRoT 102749568 based on the rotational splitting of the oscillation mode and determined the stellar parameters and helium core size using asteroseismology. These multiplet structures and the modes identification might improve our knowledge of the δ Scuti stars and offer new clues for probing the stellar interior and physical processes.

KIC 9845907 was classified as a δ Scuti star by Uytterhoeven et al. (2011). The Kepler magnitude of this star is $K_P = 11.64$ mag, and its effective temperature and radius are $T_{\rm eff} = 7936 \pm 200$ K and $R = 1.954\ R_\odot$, respectively (Brown et al. 2011). Based on the data of short-cadence (SC) observations in the Kepler field, Balona (2016) found a large number of combination frequencies in δ Scuti stars, with the

Table 1
Basic Properties of KIC 9845907

Parameters	KIC 9845907	References
K_P	11.64 mag	a
TESS magnitude	11.41 mag	c
B	11.81 mag	b
V	11.12 mag	b
J	11.03 mag	b
I	11.23 mag	b
K	10.94 mag	b
H	10.98 mag	b
g	11.67 mag	b
i	11.72 mag	b
z	11.79 mag	b
Gaia	11.57 mag	c
$M/M_\odot$	1.87 ± 0.29	c
$R/R_\odot$	1.954	b
	1.928 ± 0.067	c
$T_{\rm eff}$	7936 ± 200 K	a
	7861 ± 147 K	c
log g	4.029 ± 0.5 dex	b
	4.140 ± 0.077 dex	c
[Fe/H]	−0.039 ± 0.5 dex	b
Parallax (mas)	1.25 ± 0.01	(Gaia),d

Note. (a) Balona (2016); (b) KASOC: https://kasoc.phys.au.dk/; (c) TASOC: https://tasoc.dk; (d) Gaia (McDonald et al. 2017).

number in KIC 9845907 being 10. Some basic parameters of KIC 9845907 are listed in Table 1. In this work, we used the high-precision photometric data (including SC and Long Cadence (LC) data) provided by Kepler to further study the pulsating behavior of KIC 9845907.

2. Observations and Data Reduction

KIC 9845907 was observed by Kepler from BJD 2,454,953.539 to 2,456,424.001 (Q0–Q6, Q8–Q10, Q12–Q14, and Q16–Q17, total of 15 quarters) in 29.5 minute cadence (i.e., LC mode) and from BJD 2,454,953.529 to 2,455,833.279 (Q0, Q5.1–Q5.3, Q8.1–Q8.3, Q9.1–Q9.3 and Q10.1–Q10.3, total of five quarters) in 58.5 s cadence (i.e., SC mode). All the data were downloaded from Kepler Asteroseismic Science Operations Center (KASOC) database.[3] KASOC provides asteroseismological data from the NASA Kepler and K2 missions to astronomers. The KASOC archive classifies the pulsation stars into subcategories and δ Scuti stars corrected by Working Group 4. And KASOC provides two types data: the "raw" and corrected flux data. In this work, we converted the corrected flux to stellar magnitude and performed corrections, including eliminating the outliers and detrending the light curves. Then the mean value of each quarter was subtracted, and the rectified time series were obtained with 49551 data points in LC and 176899 in SC, spanning over about 1471 and 880 days, respectively. Figure 1 shows a section of the SC light curves of KIC 9845907, where the amplitude is about 0.1 mag.

3. Frequency Analysis

In this work, the Kepler SC data of KIC 9845907 were analyzed to search for significant frequencies using the software PERIOD04 (Lenz & Breger 2005), which allows a pre-whitening procedure spotting the frequencies through a Fourier transform (FT) of the data. The rectified light curve was fitted with the following formula:

$$m = m_0 + \sum A_i \sin(2\pi(f_i t + \phi_i)), \quad (1)$$

where m_0 is the zero point and A_i, f_i, ϕ_i are the amplitude, frequency, and phase of each mode, respectively. We chose a range of $0 < \nu < 100$ day^{-1} to search for frequencies since it covers the pulsation regime of δ Scuti stars. The upper limit of this range is well below the Nyquist frequency ($f_{Ny} = 1/(2\Delta t) = 734$ day^{-1}, where Δt is the sampling interval between consecutive points). The criterion of a signal-to-noise ratio (S/N) > 4.0 was adopted as stopping criterion for the pre-whitening process (Breger et al. 1993). The noise for each significant frequency was calculated in a box size of 2 day^{-1} centered in the extracted peak. We selected a step rate "high," corresponding to an oversampling of 20 and a frequency spacing of 0.00005683 day^{-1}. The uncertainties of all frequencies were calculated following the method provided by Montgomery & Odonoghue (1999).

A total of 85 significant frequencies with S/N > 4.0 were extracted in this work. A full list of the detected frequencies (i.e., f_1 to f_{85}), with their corresponding amplitudes and S/N, is given in Table A1 in the Appendix. Figure 2 shows the Fourier spectra of 85 significant frequencies in two different ways: one is the amplitude spectrum of KIC 9845907 in the 0–100 day^{-1} range (upper panel), and the other is the distribution of detected 85 frequencies (lower panel). As can be seen clearly in Figure 2, the frequencies with higher amplitudes were found in the range of 15–35 day^{-1}, and the other smaller peaks (i.e., f_8 and f_9) were in the range of 0–2 day^{-1}.

The δ Scuti stars usually pulsate in radial mode, and theoretically the radial modes have higher visibility than non-radial (Dziembowski 1977). Therefore, by visually inspecting the highest amplitude of the frequency spectra, we considered f_1 as a radial mode. Further evidence comes from the investigation of the pulsation constant Q (Breger & Bregman 1975), as described in Equation (2).

Radial oscillations can be estimated by the pulsation constant, Q, as given in following,

$$\log Q = \log P + \frac{1}{2}\log g + \frac{1}{10}M_{\rm bol} + \log T_{\rm eff} - 6.454, \quad (2)$$

where P is the pulsation period, g is the surface gravity, $M_{\rm bol}$ is the absolute bolometric magnitude, and $T_{\rm eff}$ is the effective temperature. And the value of $M_{\rm bol}$ can be determined below (Driling & Landolt 2000),

$$M_{\rm bol} = 42.36 - 5\log R/R_\odot - 10\log T_{\rm eff}, \quad (3)$$

where R and $R_\odot$ are the stellar radius and radius of the Sun, respectively. Therefore, the determination of the Q value depends on the accuracy of stellar parameters such as $T_{\rm eff}$, log g, and $M_{\rm bol}$. In this work, for KIC 9845907, TESS mission provides the parameters as $T_{\rm eff} = 7861.0 \pm 147$ K, $R = 1.928 \pm 0.067$ $R_\odot$, and log $g = 4.140 \pm 0.077$ dex (Stassun et al. 2019). Using these physical parameters, we found that the pulsation constant (Q) for f_1 was determined to be 0.029 ± 0.002, which is in the range of values for the fundamental and first overtone modes obtained by Lovekin & Guzik (2017) in a

[3] KASOC database: https://kasoc.phys.au.dk.

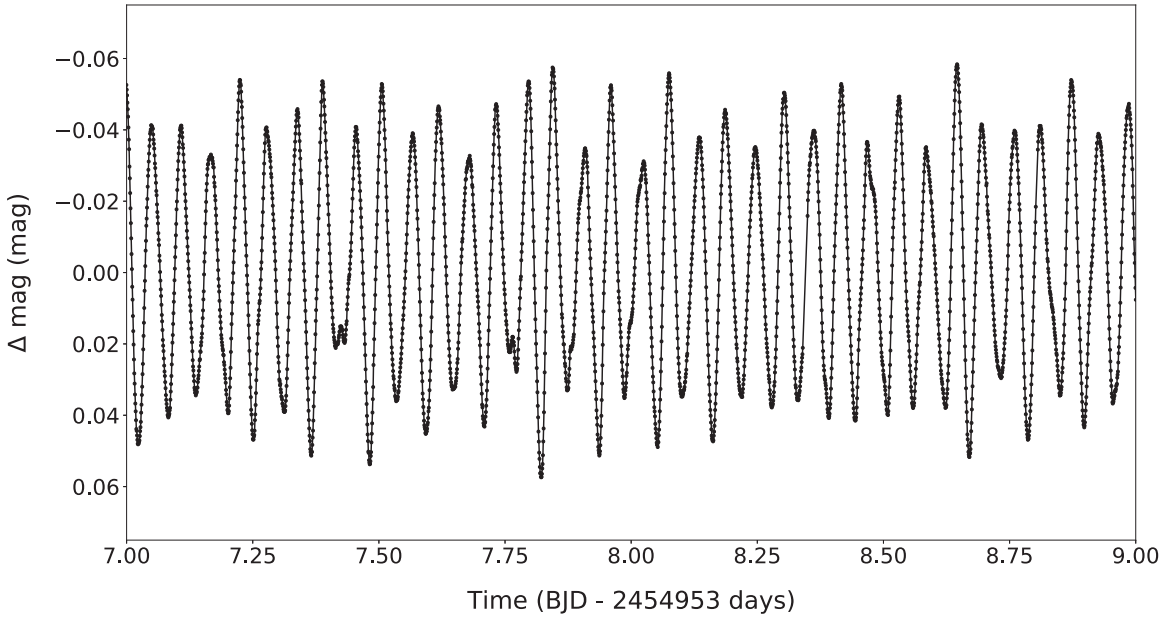

Figure 1. A 2 day section of the Kepler SC light curve of KIC 9845907. The amplitude of the light curve is about 0.1 mag. BJD is barycentric Julian date.

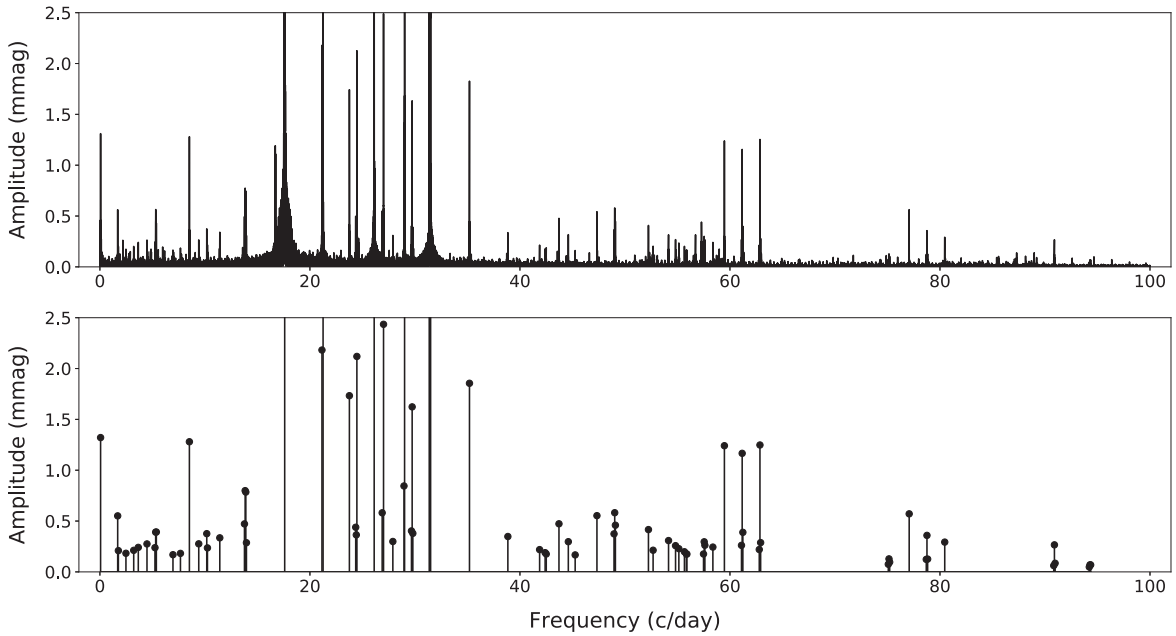

Figure 2. Amplitude spectra of KIC 9845907 using the SC data. The upper panel shows the amplitude spectrum in the 0–100 c/day range. The lower panel represents the distribution of detected 85 frequencies.

grid of rotating models representative of δ Scuti stars. Hence, we suggest f_1 is a radial mode (and further identified to be the first overtone in Section 4.6), as marked in Table A1 in the Appendix.

The frequencies $f_2 \sim f_7$ are within the frequency range of typical δ Scuti stars. They are neither combination nor harmonic frequencies, so we marked them as independent frequencies in Table A1 in the Appendix. Figure 3 shows four frequencies (f_1, f_3, f_8, and f_9), where f_1 and f_3 are two real frequencies. We found that the shape of f_8 and f_9 are similar to that of f_1 and f_3, with no multiplet structure around the peaks. This suggests that f_8 and f_9 are not instrumental artifacts. For more detailed description about the real and alias frequencies of the Kepler data, we refer to Murphy et al. (2013). Moreover, the S/N of f_8 and f_9 in SC spectrum are 28.7 and 20.0 respectively, which is far greater than the standard of S/N = 4 given by Breger et al. (1993). Hence, f_8 and f_9 are two real frequencies.

It is intriguing that 42 of the 85 frequencies form fourteen pairs of equidistant triplet structures. They are labeled as "T" in Figures 4 and 5, where the blue vertical dotted lines indicate the locations of the extracted peaks. It is clear that these equidistant frequency triplets consist of the equal spacing frequency f_8 (=0.065 day^{-1}) in Figure 4 and f_9 (=1.693 day^{-1}) in Figure 5, respectively. Moreover, f_8 and f_9 are not in the typical p-mode range of δ Scuti stars, and they are not combinations of other independent frequencies, either. Hence, we marked the frequencies f_8 and f_9 as f_{m1} and f_{m2} in Table A1 in the

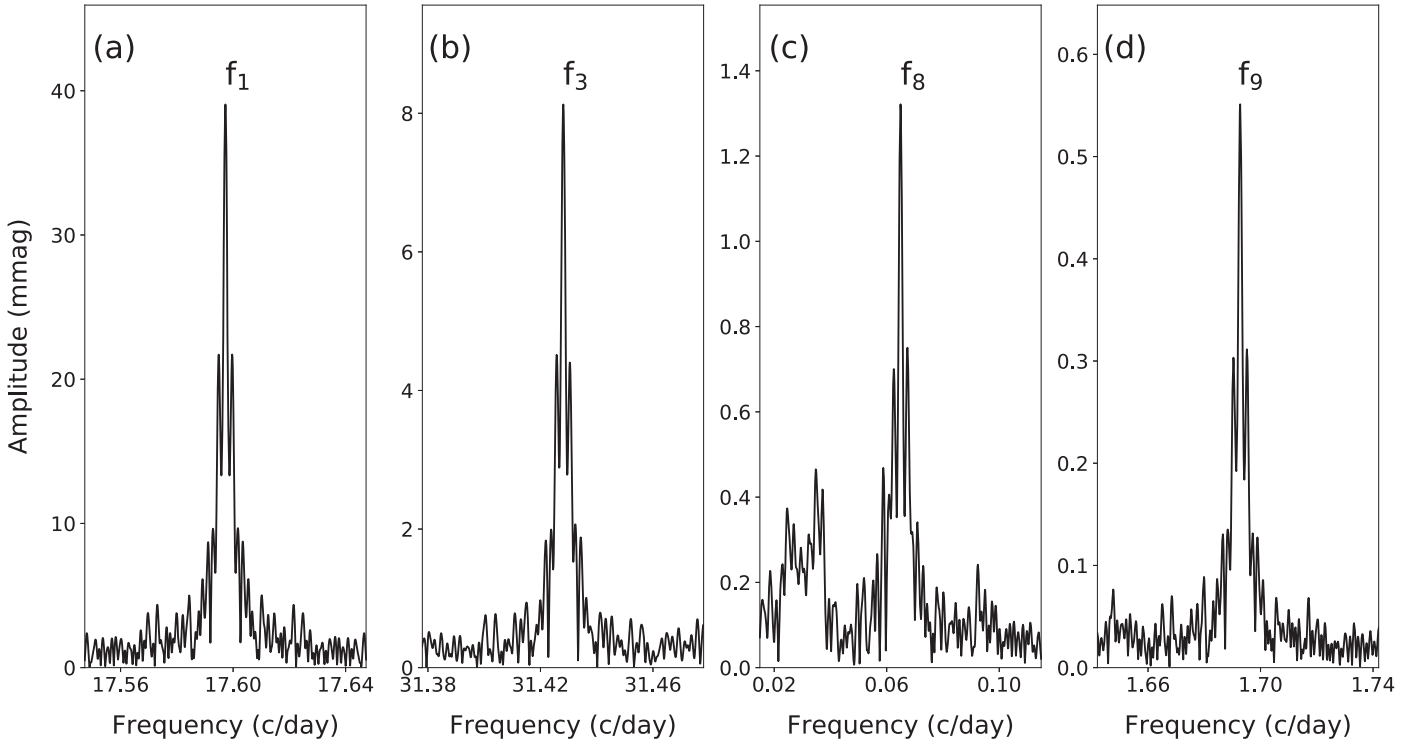

Figure 3. Typical spectra of the real frequencies. Panels (a) and (b) show two real frequencies $f_1 = 17.597\ \mathrm{day}^{-1}$ and $f_3 = 31.428\ \mathrm{day}^{-1}$; panels (c) and (d) show two modulation terms $f_8 = 0.065\ \mathrm{day}^{-1}$ and $f_9 = 1.693\ \mathrm{day}^{-1}$, respectively.

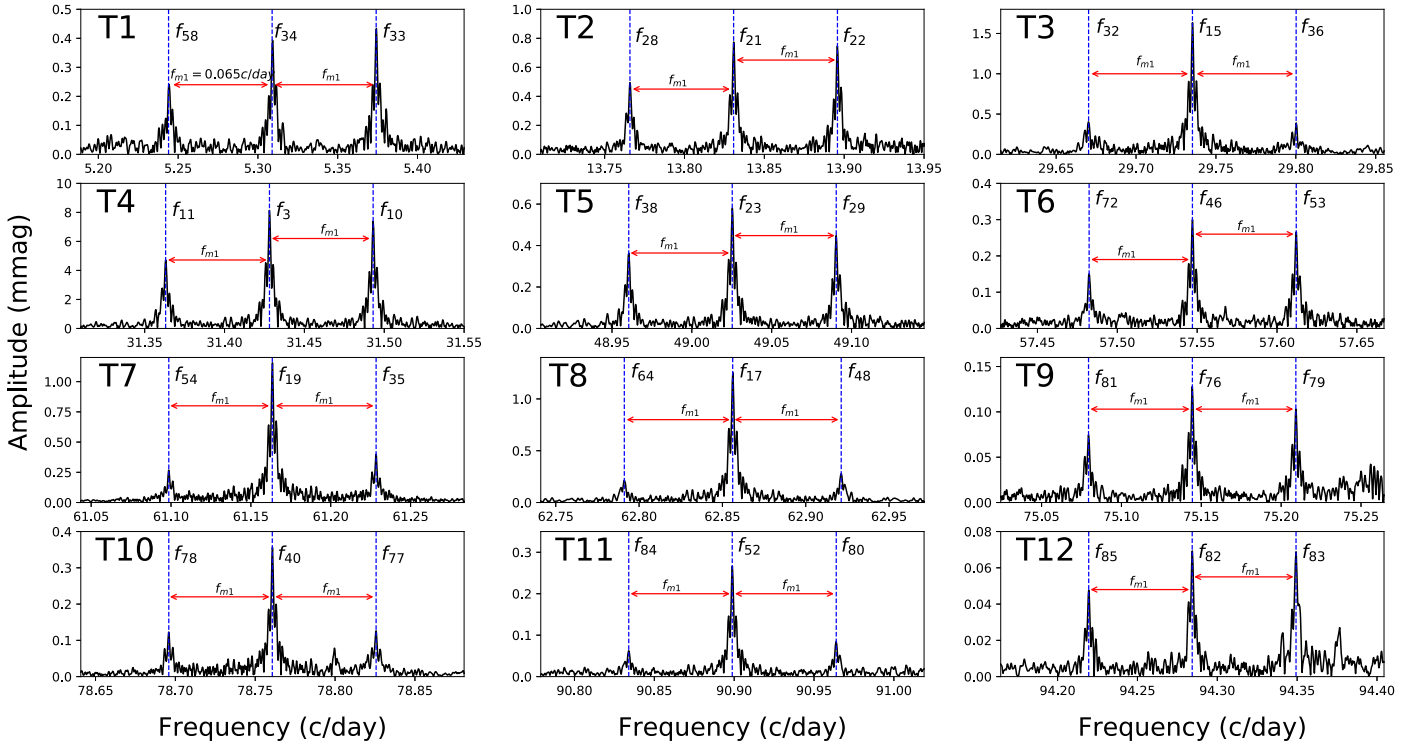

Figure 4. Twelve pairs of equidistant frequency-triplet structures in the SC spectrum of KIC 9845907. The vertical blue dotted lines indicate the locations of the detected frequencies, where $f_{m1} = 0.065\ \mathrm{day}^{-1}$ represents the spacing. We marked the triplets with f_{m1} as T1 to T12 sorted according to the increasing value of the central frequency.

Appendix, respectively. In Table 2, we marked the triplets with the equidistant frequency f_{m1} as T1 to T12 and the group with f_{m2} as T13 and T14, sorted according to the increasing value of the central frequency, respectively.

Moreover, we also found two pairs of quintuplet structures ("Q") in the SC frequency spectra. In Table 3, we marked the two pairs as Q1 and Q2, sorted according to the increasing value of the central frequency. Figure 6 shows these two pairs

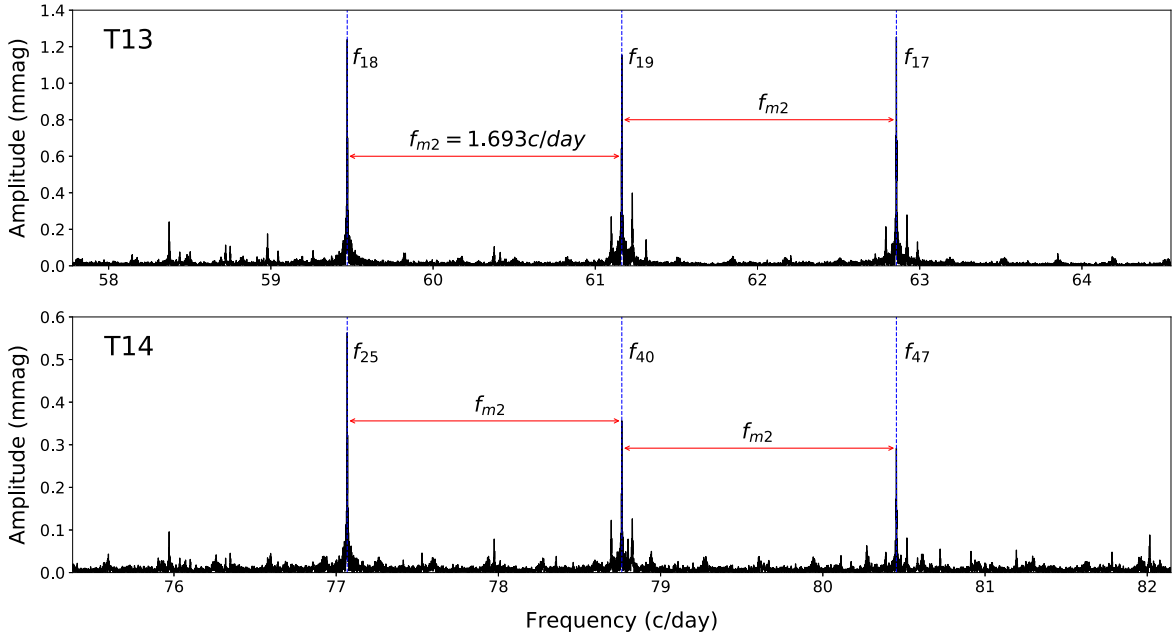

Figure 5. Two pairs of equidistant frequency-triplet structures in SC spectrum of KIC 9845907. The vertical blue dotted lines indicate the locations of frequencies, where $f_{m2} = 1.693$ day^{-1} represents the equally spaced frequency. We marked the triplets with f_{m2} as T13 and T14 according to Table 2.

Table 2
Dominant Frequencies of the "T" Family in the SC Data (Denoted by f_i)

f_i	Frequency (day^{-1})	Identification	Comment	f_i	Frequency (day^{-1})	Identification	Comment
8	0.0649(1)	f_8	f_{m1}	9	1.6927(5)	f_9	f_{m2}
34	5.3091(2)	f_{34}	T1	17	62.8562(6)	f_{17}	T8
33	5.3741(4)	$f_{34} + f_{m1}$	T1	48	62.9211(7)	$f_{17} + f_{m1}$	T8
58	5.2443(3)	$f_{34} - f_{m1}$	T1	64	62.7913(6)	$f_{17} - f_{m1}$	T8
21	13.8308(6)	f_{21}	T2	76	75.1444(1)	f_{76}	T9
22	13.8957(6)	$f_{21} + f_{m1}$	T2	79	75.2092(7)	$f_{76} + f_{m1}$	T9
28	13.7659(5)	$f_{21} - f_{m1}$	T2	81	75.0793(9)	$f_{76} - f_{m1}$	T9
15	29.7353(7)	f_{15}	T3	40	78.7607(8)	f_{40}	T10
36	29.8002(8)	$f_{15} + f_{m1}$	T3	77	78.8256(8)	$f_{40} + f_{m1}$	T10
32	29.6703(6)	$f_{15} - f_{m1}$	T3	78	78.6958(8)	$f_{40} - f_{m1}$	T10
3	31.42813(3)	f_3	T4	52	90.8987(7)	f_{52}	T11
10	31.4930(3)	$f_3 + f_{m1}$	T4	80	90.9639(1)	$f_{52} + f_{m1}$	T11
11	31.3631(1)	$f_3 - f_{m1}$	T4	84	90.8339(8)	$f_{52} - f_{m1}$	T11
23	49.0254(5)	f_{23}	T5	82	94.2843(9)	f_{82}	T12
29	49.0903(1)	$f_{23} + f_{m1}$	T5	83	94.3493(4)	$f_{82} + f_{m1}$	T12
38	48.9605(1)	$f_{23} - f_{m1}$	T5	85	94.2194(9)	$f_{82} - f_{m1}$	T12
46	57.5470(3)	f_{46}	T6	19	61.1635(1)	f_{19}	T13
53	57.6120(4)	$f_{46} + f_{m1}$	T6	17	62.8562(6)	$f_{19} + f_{m2}$	T13
72	57.4821(2)	$f_{46} - f_{m1}$	T6	18	59.4707(5)	$f_{19} - f_{m2}$	T13
19	61.1635(1)	f_{19}	T7	40	78.7607(8)	f_{40}	T14
35	61.2284(1)	$f_{19} + f_{m1}$	T7	47	80.4535(8)	$f_{40} + f_{m2}$	T14
54	61.0984(9)	$f_{19} - f_{m1}$	T7	25	77.0680(3)	$f_{40} - f_{m2}$	T14

Note. "T", f_{m1}, and f_{m2} represent equidistant frequency-triplet structures and two equally spaced frequencies, respectively. We marked the equidistant frequency triplets of the group with f_{m1} as T1 to T12 and the group with f_{m2} as T13 and T14, sorted according to the increasing value of the central frequency, respectively.

of quintuplet structure with the blue dotted lines representing the location of each extracted frequency. It is clear that the side peaks around f_{19} (and f_{40}) in the frequency spectra of KIC 9845907 have two pairs of uniformly spaced triplets with intervals of $f_{m1} = 0.065$ day^{-1} and $f_{m2} = 1.693$ day^{-1}, i.e., Q1 includes T7 and T13, while Q2 includes T10 and T14, respectively. To see clearly the central triplets with f_{m1} in Figure 6, we refer to T7 and T10 in Figure 4. Note that four out of fourteen pairs of triplets can form quintuplet structures, which is very interesting and recognized for the first time in δ Scuti stars. We suggest these phenomena deserve further study, and we give a discussion on the possible explanations in Section 4.

4. Discussion

In recent years, more and more regular frequency spacings have been found in several δ Scuti stars, thanks to the high-

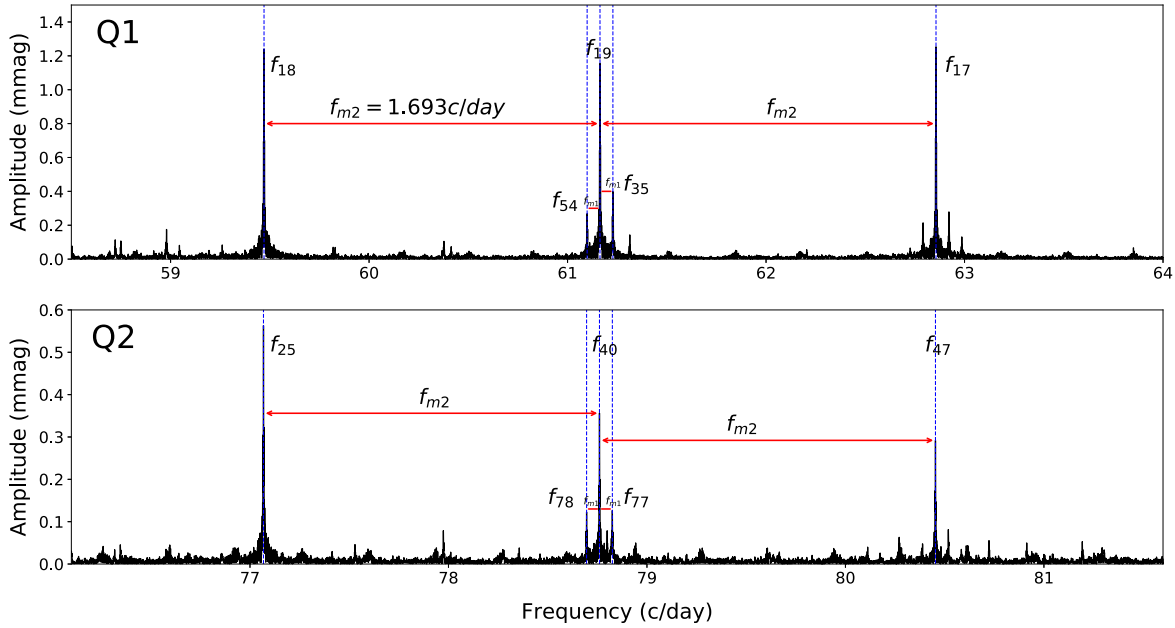

Figure 6. Two pairs of quintuplet structures in SC spectrum of KIC 9845907. The vertical blue dotted lines indicate the locations of frequencies. We marked the two pairs as Q1 (upper panel) and Q2 (lower panel), sorted according to the increasing value of the central frequency, respectively. The intervals from the side peaks to the center are marked with $f_{m1} = 0.065$ day^{-1} and $f_{m2} = 1.693$ day^{-1}, respectively. In the upper and lower panels, the zoomed-in view of the central triplets can be seen in Figure 4 (i.e., T7 and T10) for clarity.

Table 3
Dominant Frequencies of the "Q" Family in the SC Data (Denoted by f_i)

f_i	Frequency (day^{-1})	Identification	Comment	f_i	Frequency (day^{-1})	Identification	Comment
19	61.1635(1)	f_{19}	Q1	40	78.7607(8)	f_{40}	Q2
17	62.8562(6)	$f_{19}+f_{m2}$	Q1	47	80.4535(8)	$f_{40}+f_{m2}$	Q2
35	61.2284(1)	$f_{19}+f_{m1}$	Q1	77	78.8256(8)	$f_{40}+f_{m1}$	Q2
54	61.0984(9)	$f_{19}-f_{m1}$	Q1	78	78.6958(8)	$f_{40}-f_{m1}$	Q2
18	59.4707(5)	$f_{19}-f_{m2}$	Q1	25	77.0680(3)	$f_{40}-f_{m2}$	Q2

Note. "Q" represents quintuplet structures. We marked the two pairs as Q1 and Q2, sorted according to the increasing value of the central frequency, respectively.

precision continuous photometric data provided by space telescopes. The identification of these pulsation frequency modes provides us with new clues to study these variable stars. For example, Bedding et al. (2020) studied 60 δ Scuti stars with regular frequency spacings and enabled mode identification by comparing with theoretical models.

The most interesting features for KIC 9845907 in this study are the regular frequency spacings, including equidistant frequency-triplet and quintuplet structures, with frequency intervals of $f_{m1} = 0.065$ day^{-1} and $f_{m2} = 1.693$ day^{-1}. Two pairs of triplet structure overlap to form a quintuplet structure, hence, with the same frequency spacings (of f_{m1} and f_{m2}). To explore the nature of these frequency structures, we first need to consider whether they arise from the known instrumental effects of Kepler, including: (1) the frequency of Kepler orbital period $f_{\rm orb} = 0.00268$ day^{-1}, (2) the momentum desaturation of the reaction wheel $f_{\rm reaction} = 0.336$ day^{-1} (Van Cleve & Caldwell 2016), (3) the frequency induced by the data downlink $f_{\rm downlink} = 0.031$ day^{-1}, and (4) that of Kepler rotation $f_{\rm rot} = 0.011$ day^{-1}. The Rayleigh frequency resolution of the SC data is 0.001136 day^{-1} for KIC 9845907. We found that the value of f_{m1} was not equal to (1) and (2) within the Rayleigh frequency resolution; therefore, these two instrumental effects are excluded first. For the frequency $f_{\rm downlink}$ (=0.031 day^{-1}), f_{m1} is about twice of it. To verify if f_{m1} is caused by the data downlink, we only used a part of 32 day ($=1/f_{\rm downlink}$) data to extract frequencies and still detected the f_{m1}, so this instrumental effect is excluded. For the frequency $f_{\rm rot}$, f_{m1} seems to be 6 times of it. If the equidistant structure in the spectra is caused by the instrument effect, the height of the side lobe frequencies on both sides of the peak should be the same. But the triplets with f_{m1} (T1–T12) of KIC 9845907 are not like this. In addition, instrumental effect should be applied at all significant independent frequencies. For KIC 9845907, we only detected the equidistant frequency-triplet structure at one independent mode (i.e., f_3) and none at the others. And when using the software PERIOD04 for frequency extraction, we did not detect 1–5 times of the Kepler rotation frequency; these signals should be stronger than $6f_{\rm rot}$. Hence, $f_{m1} \approx 6f_{\rm rot}$ is probably a coincidence. For f_{m2}, we found that none of the known frequencies of instrumental effects from Kepler were equal to it within the Rayleigh frequency resolution.

4.1. Beating?

Breger & Bischof (2002) found that pairs of close-frequency pulsation modes with spacings less than 0.01 day^{-1} were

common by studying seven well-known δ Scuti stars. Breger et al. (2009) found that pulsation frequencies in δ Scuti stars are not distributed randomly and that many non-radial modes had frequencies near radial mode frequencies. These regularities were explained by mode trapping in the stellar envelope (Dziembowski & Krolikowska 1990), which explained the regularities in the amplitude spectrum in the δ Scuti star FG Vir (Breger et al. 2009).

However for KIC 9845907, the spacings of the close frequencies are $f_{m1} = 0.065$ day^{-1} and $f_{m2} = 1.693$ day^{-1}, both of which are much larger than the typical value (i.e., 0.01 day^{-1}) in Breger & Bischof (2002). Moreover, there is no unresolved peak around the dominant frequencies in the residuals, and the overall distribution of the residuals is typical of noise. Hence, the equidistant triplet structures of KIC 9845907 are unlikely caused by beating.

4.2. Blazhko Effect?

Equidistant structures are often shown in the Fourier spectra of the Blazhko RR Lyrae stars, and the interval of the triplets is the same as the modulation frequency, which can be directly detected (Jurcsik et al. 2005; Kolenberg et al. 2006). For KIC 9845907 in our case the equidistant quintuplet structures in the SC spectrum are similar to that in Blazhko RR Lyr stars, and two modulation frequencies are detected clearly. These features imply that the quintuplet structures in KIC 9845907 may be related to the Blazhko effect.

Using the high-precision photometric data provided by Kepler, Blazhko-like effect has been found in some δ Scuti stars. For example, the double-mode HADS star KIC 10284901 shows two pairs of quintuplet structure, and its analysis suggests that the modulation term of the quintuplet structures might be related to the Blazhko effect (Yang & Esamdin 2019). The main characteristic of this effect is that the quintuplet structures appear around the fundamental and first overtone pulsation modes (i.e., F0 and F1). However, for KIC 9845907, the two pairs of quintuplet structures are not the case, that is to say, they appear around other modes, which are not similar to that in KIC 10284901. Moreover, in KIC 10284901 the ratio of the two modulation frequencies (f_{m1} and f_{m2}) is nearly 1:2. However, in the case of KIC 9845907, the ratio of the two modulation frequencies ($f_{m1} = 0.065$ day^{-1} and $f_{m2} = 1.693$ day^{-1}) of the quintuplet structures is seriously deviated from 1:2. From these aspects, we rule out the possibility that the quintuplet structures are caused by the Blazhko effect, as observed in RR Lyrae stars.

4.3. Combination Mode Hypothesis?

For the equidistant frequency-triplet structures in δ Scuti stars, Breger & Kolenberg (2006) provided an explanation named the "Combination Mode Hypothesis." In this hypothesis, the highest amplitude mode ν_1 and a real second mode ν_2 are excited; then, the harmonics as well as the combinations of ν_1 and ν_2 may also occur. The simplest combination (e.g., $\nu_3 = \nu_2 - \nu_1$) is usually observed, and then a pair of frequency-triplet (i.e., ν_3, ν_1, and ν_2) is formed around ν_1 in the frequency spectra.

To test this possibility, we chose the triplet structure T4 (i.e., f_3, f_{10} and f_{11}) in KIC 9845907 for further analysis since the amplitude of the central component (i.e., f_3) of T4 is the strongest. Under this hypothesis, the right component $f_{10} = 31.493$ day^{-1} in the equidistant frequency-triplet structure in the SC spectrum of KIC 9845907 is considered as a new independent mode. However, the ratio of $f_1/f_{10} = 0.559$ is not within the typical range of the continuous radial period ratios (Stellingwerf 1979). This seems to rule out the possibility that f_{10} belongs to a radial mode. If f_{10} is assumed to be a non-radial mode, it would split into $2\ell + 1$ frequencies when the star rotates. However, it is not like this case, either, as f_{10} does not exhibit any splitting structure in the frequency spectra. Consequently, f_{10} in KIC 9845907 is not an independent mode.

4.4. Nonlinear Mode Coupling?

Different nonlinear effects can generate combination frequencies in the spectrum of pulsating stars (Bowman et al. 2016). Combination frequencies are common in δ Scuti stars, and it is of great importance to identify which peak is combination frequency and which is a real frequency as it can greatly simplify the frequency spectra (Kurtz et al. 2015). However, combination frequencies differ from the mode coupling, which are excited by the resonant interaction of pulsation modes in stars. Coupled frequencies are grouped into two families: child and parent modes, and this coupling of modes promotes energy exchange between different modes of the family (Nowakowski 2005). The frequencies and amplitudes of pulsating modes change with time due to nonlinear mode coupling. Hence, when we distinguish coupled modes from combination frequencies, we need to study the changes of frequency, amplitude, and phase for each family.

In the theory of nonlinear mode coupling, the child and parent modes are directly related in frequency and phase. The way to distinguish the parent and coupled modes is to examine the correlations in amplitude variability. Breger & Montgomery (2014) investigated the dominant modes excited in KIC 8054146, which they called the T family. They computed changes of amplitudes and phases and correlations between different frequencies that show qualitative similarities between Triplets 1 and 2 (see the Figures 2 and 3 in Breger & Montgomery 2014). Finally, they identified the coupled modes of the T family in KIC 8054146. In this work, following the method by Breger & Montgomery (2014), we investigated the correlations in amplitude and phase variability between different dominant pairs of equidistant triplet structures.

The 4 yr of available LC data of KIC 9845907 allow us to examine the correlations of the amplitude and phase changes of the dominant frequencies and help to detect their physical relationship and origin. This near-continuous LC data from Q0 to Q17 span 1471 days in total. To make a compromise between studying short-term amplitude and phase changes and obtaining excellent frequencies from larger time intervals, a 75 day interval was chosen. In the next step, average frequencies covering the entire Q0–Q17 quarters were determined. Each value of the frequencies is labeled in the upper left corner of each panel in Figure 7. Using these average frequencies, the amplitudes and phase were calculated for different modes in each 75 day interval. This is shown in Figures 7 and 8, respectively. In the last row we also show the results for modes at $f_{m1} = 0.065$ day^{-1} and $f_1 = 17.597$ day^{-1} for comparison. The error bars are also plotted, obtained by Monte Carlo simulation in PERIOD04.

Figure 7 shows the amplitude variations of KIC 9845907. The panels in the top three rows represent the low, central, and high components (from top to bottom) of T2 (left) and T4

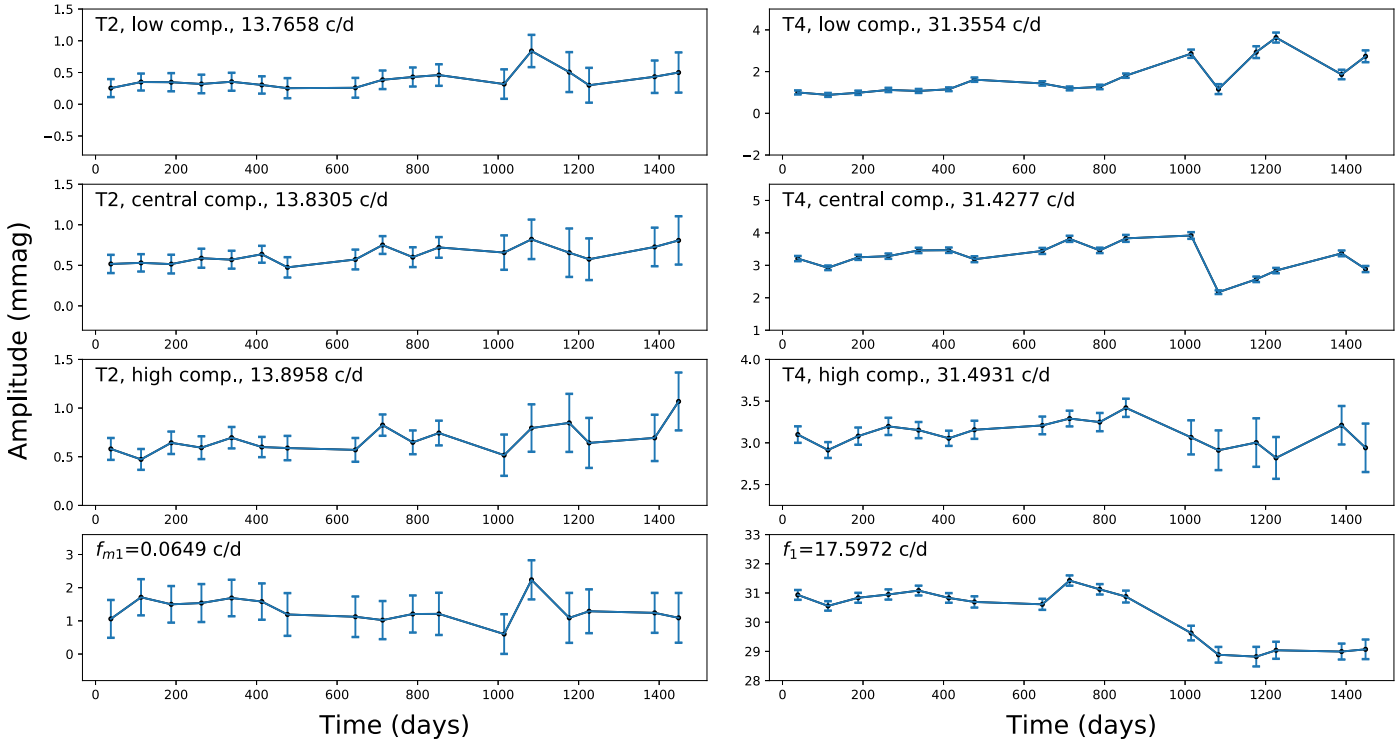

Figure 7. Amplitude variations of the components of Triplet 4 (T4) and Triplet 2 (T2). Two dominant frequencies, f_{m1} and f_1, are also shown for comparison.

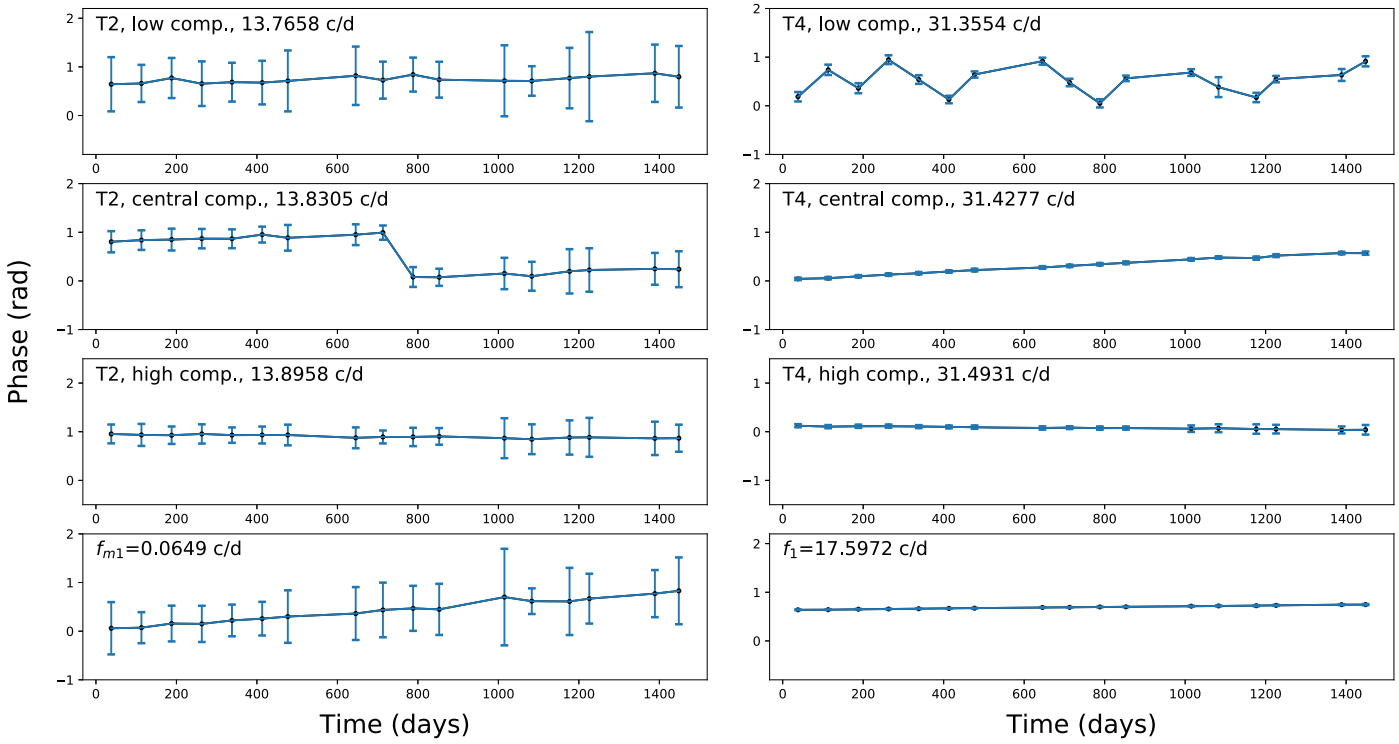

Figure 8. The same as in Figure 7 but for phase variations of the modes.

(right), respectively. The bottom panels are the amplitude variations of f_{m1} and f_1, respectively. For the three components of T2, before 1000 days, the amplitude variations were relatively stable but then changed significantly (i.e., increasing or decreasing). However, for T4, the changes occur much earlier, at the time of 700 days. For f_{m1}, the amplitude change is relatively stable as a whole without obvious changes, and the frequency f_1 breaks the stability after 700 days. Then it tends to be stable after a significant decline. We note there is no similarity and synchronization of amplitude variations between T2 and T4, which is not similar to the case of KIC 8054146.

Figure 8 shows the phase variations of KIC 9845907 with the panels labeled the same as in Figure 7. For the low and high components in T2, there is no obvious change in the overall

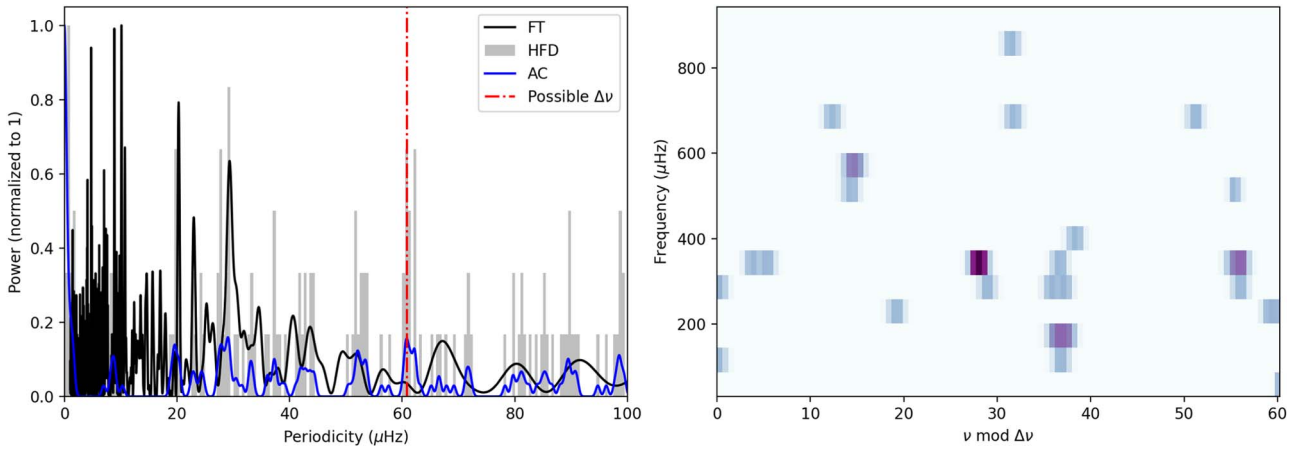

Figure 9. In the left panel, the black, gray, and blue lines represent the Fourier transform (FT), the histogram of frequency differences (HFD), and the autocorrelation function (AC), respectively, using the methodology of García Hernández et al. (2013) and Ramón-Ballesta et al. (2021). The red dotted–dashed line indicates the possible value of $\Delta\nu = 5.25$ day^{-1}. The right panel shows the echelle diagram of the frequencies. The value of 60.8 μHz is used for the plot.

phase, but the central component has a significant decline after 600 days. For the phase variations of T4, the three components have different changes: the low component can increase and/or decrease, while the central is gradually increasing, and the high is relatively stable. f_{m1} and f_1 are in a slowly increasing and stable state, respectively. Therefore, there is no similarity and synchronization between T2 and T4, either.

We also made a further quantitative calculation following the method provided by Breger & Montgomery (2014; see their Equation (5)) and confirmed that T4 is not the result of mode coupling between T2 and the radial mode f_1. We conclude that there is no sufficient evidence so far to support the possibility that the triplets are caused by nonlinear mode coupling.

4.5. Large Separation?

Observations have shown that many δ Scuti stars have regular frequency spacings in their rich pulsation spectra. There have been several studies searching for large separations (e.g., García Hernández et al. 2013; Bedding et al. 2020). This development follows the establishment of the relationship between the large separation in the low-order regions and the average density of the star from the modelings (e.g., Suárez et al. 2014) and the observations (García Hernández et al. 2015, 2017).

We used the methodology provided by García Hernández et al. (2013) and Ramón-Ballesta et al. (2021) to determine the large separation, $\Delta\nu$, of KIC 9845907. Three techniques were applied to the frequencies: (1) the FT, (2) the autocorrelation function (AC), and (3) the histogram of frequency differences (HFD). The result of KIC 9845907 is shown in the left panel of Figure 9, where the black, gray, and blue lines represent FT, HFD, and AC, respectively. All these transformations have been made using just the 30 highest amplitude modes and discarding those frequencies below 5 day^{-1}, and the amplitudes of the frequencies have been normalized to unity when doing all these transformations. If there exists a periodicity in the form of Dirac comb, then we will see a peak corresponding to $\Delta\nu$ and others at the multiples in the AC (2 $\Delta\nu$, 3$\Delta\nu$, etc). On the contrary, in the FT we expect to find $\Delta\nu$ and the submultiples ($\Delta\nu/2$, $\Delta\nu/3$, etc), just because of how the transform works. In conclusion, in the FT, we could not find $\Delta\nu$ but just the submultiples ($\Delta\nu/2$ and/or $\Delta\nu/3$) while $\Delta\nu$ appears in the AC and HFD.

For KIC 9845907, the left panel of Figure 9 shows a peak at around 5.25 day^{-1} (=60.8 μHz, the red dotted–dashed line) in the AC and HFD. However, in the FT, it does not show a peak around $\Delta\nu$, but we can see $\Delta\nu/2$ (the high peak around 30 μHz) and $\Delta\nu/3$ (the high peak around 20 μHz). The absence of the peak of $\Delta\nu$ in the FT is expected, although to identify it at least one submultiple is mandatory (e.g., Garcia Hernandez et al. 2009), and the presence of more submultiples indicates that the possible value of large separation ($\Delta\nu$) is around 60.8 μHz and not 30 μHz. Moreover, the large separation (~5.1 day^{-1}) we obtained from the models (see Section 4.6 for more detail) is close to the observed one.

Using this value (60.8 μHz), the echelle diagram is shown in the right panel of Figure 9. Some frequencies appear darker as they are composed of two very close frequencies. It can be seen that the distribution of these modes is irregular, with additional ridges at various angles, indicating that the analysis method of using simple pulsation spectra (with $\ell = 0$ and 1) is insufficient to interpret this echelle diagram. In fact, this phenomenon also appears in other δ Scuti stars. For example, in four δ Scuti stars (i.e., HD 37286, SAO 150524, TYC 8533-329-1, and β Pic), complex patterns were also detected in the echelle diagrams. Bedding et al. (2020) concluded that the complex echelle diagram might be related to the azimuthal order m. Therefore, only using the large separation 60.8 μHz cannot provide a reasonable explanation for the triple structures and the rich spectrum for KIC 9845907.

4.6. Stellar Rotational Splitting?

The theory of stellar oscillations in the spherical approximation states that each oscillation mode can be characterized by three spherical harmonics: number of nodes along the radius direction n, the spherical harmonic degree ℓ, and the azimuthal order m. If a star is rotating, the rotation can cause the non-radial oscillation mode to split into $2\ell + 1$ components in the inertial frame. And at first order in the perturbation theory, in a slowly rotating star, the $2\ell + 1$ frequencies of the non-radial mode are separated by almost the same spacing, corresponding to an average rotation frequency. In addition, if a star is in a binary system, the binarity would split all the modes, even the radial, because of the motion around the center of masses (Shibahashi & Kurtz 2012). This is not the case for KIC 9845907, as the frequency f_1, a radial order and the highest

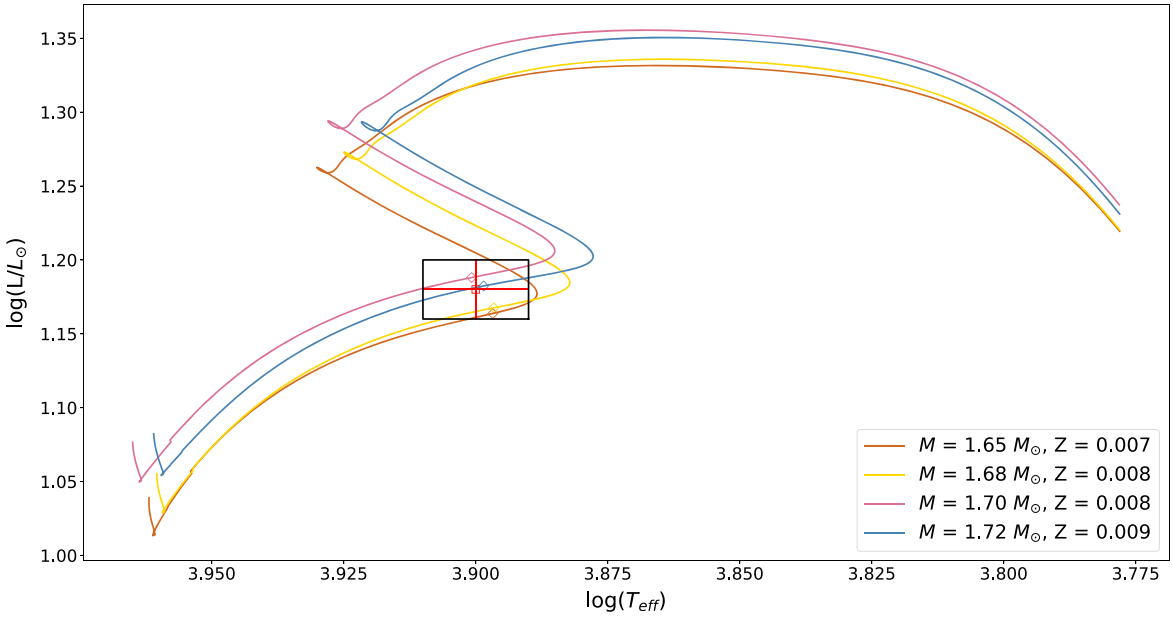

Figure 10. Evolutionary tracks from the zero-age MS to the post-MS for the four candidate models, as listed in Table 4. The black rectangle marks the 1σ error box of the effective temperature $T_{\rm eff}$ and the luminosity L, while the diamonds mark the minimum χ^2 for each specific model by fitting the observed $f_1 = 17.597$ day^{-1} and $f_3 = 31.428$ day^{-1} with the theoretical values.

Table 4
Candidate Models with $\chi^2 \leqslant 0.0056$

Mass ($M_\odot$)	Z (dex)	$T_{\rm eff}$ (K)	$\log(L/L_\odot)$	f_1 (ℓ, n) (c days^{-1})	f_3 (ℓ, n) (c days^{-1})	χ^2
1.65	0.007	7885	1.164	17.5405 (0,2)	31.4926 (1,6)	0.0037
1.68	0.008	7881	1.168	17.5386 (0,2)	31.4876 (1,6)	0.0035
1.70	0.008	7958	1.188	17.5364 (0,2)	31.4752 (1,6)	0.0031
1.72	0.009	7916	1.182	17.5170 (0,2)	31.4582 (1,6)	0.0037

Note. (ℓ, n) are the spherical harmonic degree and the radial order of the model frequency, respectively.

amplitude peak, did not split, implying that this star should be a single star. Hence, the rotational splitting of a single star was considered to account for the triplet structures in KIC 9845907. In T1–T14, the highest amplitude of the middle peak is f_3 (in T4), which is an independent frequency, while all other middle peaks are combination frequencies, so only T4 will be discussed in detail in this section. To verify whether T4 is caused by the rotational splitting of f_3, we used asteroseismic models to estimate the value of l for f_3.

We constructed a grid of evolutionary models of KIC 9845907 and calculated their corresponding frequencies using the submodule "*pulse_adipls*" of the Modules for Experiments in Stellar Astrophysics (MESA v10398; Paxton et al. 2011, 2013, 2015, 2018, 2019). In the grid, the stellar mass ranges from 1.5 $M_\odot$ to 2.0 $M_\odot$ with a step of 0.01 $M_\odot$, and metallicities range from 0.006 to 0.015 with a step of 0.001. For the helium abundance Y, we adopted $Y = 0.249 + 1.33\,Z$ as a function of Z. In addition, the classical mixing length theory of Böhm-Vitense (1958) with $\alpha = 1.9$ (Paxton et al. 2013) was adopted. Each model in the above grid was evolved from the zero-age MS to the post-MS stage to calculate the pulsation frequencies of $\ell = 0$, 1, and 2. Then, by using the method from Chen & Li (2019; i.e., Equation (5), χ^2 method), the goodness of fit can be obtained by comparing model frequencies with the observed frequencies f_1 and f_3. To select the best-fitting models, we chose a threshold of $\chi^2 = 0.0056$ (corresponding to about 5 times the frequency resolution $1/\Delta$T) and limited the model results by combining the observed effective temperature (7700 K $< T_{\rm eff} <$ 8100 K, covering the values given by Kepler and TESS) and luminosity ($14.45 < L/L_\odot < 15.85$, estimated from Gaia parallax). Finally, four candidate models are obtained, as described in the following.

Figure 10 shows the evolutionary tracks of the four candidate models on the H-R diagram, where different colored lines represent different models. The black rectangle marks the 1σ error box of the effective temperature $T_{\rm eff}$ and the luminosity L, while the diamonds denote the seismic models that can best reproduce the frequencies of the two modes f_1 and f_3. Table 4 lists the parameters of the four candidate models. The (ℓ, n) of f_1 of all candidate models is (0, 2), indicating that f_1 is the first overtone, which makes KIC 9845907 a δ Scuti star with the first overtone as the dominant frequency. For f_3, the (ℓ, n) of all candidate models is (1, 6), indicating that f_3 is a non-radial oscillation mode with $\ell = 1$. Then, it may result into $2\ell + 1$ (i.e., 3) frequencies due to the rotational splitting, as shown in T4. Thus, we suggest equidistant triplet structures with $f_{m1} = 0.065$ day^{-1} (i.e., T1–T12) might be related to rotational splitting. For the T13 and T14 (as well as Q1 and Q2), we suggest that they are derived from combination of independent frequencies (see Table A1 in the Appendix). The mode identification for other independent frequencies deserves

a thorough investigation, which is, however, beyond the scope of this paper.

With the value of the rotational splitting (i.e., $f_{m1} = 0.065$ day^{-1}), the rotational period of KIC 9845907 can be calculated, i.e., $P_{\rm rot} = 7.69$ day. Using the formula $v_{\rm rot} = \frac{2\pi R}{P_{\rm rot}}$ and the radius of KIC 9845907 provided by TESS, $R = 1.928 \pm 0.067\ R_{\odot}$ (Stassun et al. 2019), the rotation rate of KIC 9845907 at the equator can be obtained, i.e., $v_{\rm rot}$ ($v \sin i$) $= 12.70\ ^{+0.42}_{-0.46}$ km s^{-1}. Note that our result is similar to the rotational velocity (10.859 km s^{-1}) measured by Xiang et al. (2022) using low-resolution spectra and the analysis by Niemczura et al. (2017) using high-resolution spectroscopy. When compared with the average rotation ($\sim$150 km s^{-1}) of the typical δ Scuti stars (Breger 2000), the rotation of KIC 9845907 suggests that it is a slow rotator. This is also in agreement with a symmetric structure of the split frequencies.

5. Summary

Based on the high-precision time-series photometric SC data from the Kepler, we analyzed the pulsations of KIC 9845907 and detected 85 significant frequencies (see Figure 2 and Table A1 in the Appendix), including the radial frequency $f_1 = 17.597$ day^{-1}, the non-radial frequency $f_3 = 31.428$ day^{-1} ($\ell = 1$), and two modulation terms ($f_{m1} = 0.065$ day^{-1} and $f_{m2} = 1.693$ day^{-1}). In addition, f_1 is the first overtone mode, which makes KIC 9845907 a δ Scuti star with the first overtone as the dominant frequency.

Although equidistant frequency-triplet structure has been seen in other δ Scuti stars, the number of such occurrences in KIC 9845907 is unusual (fourteen pairs; see Figures 4 and 5 and Table 2). The modulation frequencies do not arise from known instrumental effects of Kepler. We also found quintuplet structures in the frequency spectra in KIC 9845907 (see Figure 6 and Table 3). We discussed several potential explanations, i.e., beating, the Blazhko effect, combination mode hypothesis, nonlinear mode coupling, large separation, and stellar rotational splitting for the equidistant structures in frequency spectra. Numerical results of asteroseismic models indicate this modulation with f_{m1} might be related to the rotational splitting. We suggest searching for more δ Scuti stars with triplet and/or quintuplet structures; using high-precision space photometry would be helpful to explore its origin.

Acknowledgments

We would like to thank the Kepler science team for providing such excellent data. This research is supported by the program of the National Natural Science Foundation of China (grant Nos. U1938104 and 12003020). A.G.H. acknowledges support from "FEDER/Junta de Andalucía-Consejería de Economía y Conocimiento" under project E-FQM-041-UGR18 by Universidad de Granada and from the Spanish State Research Agency (AEI) project PID2019-107061GB-064.

Appendix

In Table A1, we listed the 85 extracted frequencies (i.e., f_1 to f_{85}), their corresponding amplitudes, and S/N, as well.

Table A1
Multi-frequency Solution of the SC Light Curves of KIC 9845907 (Denoted by f_i)

f_i	Frequency (day^{-1})	Amplitude (mmag)	S/N	Comment
	Independent frequencies			
1	17.597272(1)	39.049	99.4	radial
2	26.11889(7)	9.780	82.3	Independent
3	31.42813(3)	8.127	56.1	non-radial
4	21.2524(1)	5.606	67.8	Independent
5	29.0141(5)	3.219	51.2	Independent
6	27.0100(6)	2.435	22.8	Independent
7	24.4713(8)	2.119	39.7	Independent
8	0.0649(1)	1.321	28.7	f_{m1}
9	1.6927(5)	0.551	20.0	f_{m2}
	Combination frequencies			
10	31.4930(3)	7.418	40.9	$f_3 + f_8$
11	31.3631(1)	4.787	26.1	$f_3 - f_8$
12	21.1456(6)	2.182	23.1	$f_2 + 2f_5 - 2f_3 - 2f_8$
13	35.1945(4)	1.855	54.7	$2f_1$
14	23.7585(6)	1.733	31.5	$f_2 + f_5 - f_3 - f_8$
15	29.7353(7)	1.623	25.1	$f_3 - f_9$
16	8.5216(2)	1.280	39.6	$f_2 - f_1$
17	62.8562(6)	1.248	58.3	$2f_3$
18	59.4707(5)	1.241	54.5	$2f_3 - 2f_9$
19	61.1635(1)	1.166	53.2	$2f_3 - f_9$
20	28.9573(1)	0.845	13.6	$f_5 - f_8$
21	13.8308(6)	0.799	18.9	$f_3 - f_1$
22	13.8957(6)	0.785	18.2	$f_3 - f_1 + f_8$
23	49.0254(5)	0.582	27.9	$f_1 + f_3$
24	26.8801(3)	0.581	23.8	$f_6 - f_8$
25	77.0680(3)	0.571	45.8	$f_1 + 2f_3 - 2f_9$
26	47.3326(5)	0.553	29.0	$f_1 + f_3 - f_9$
27	43.7161(6)	0.473	24.6	$f_1 + f_2$
28	13.7659(5)	0.472	12.1	$f_3 - f_1 - f_8$
29	49.0903(1)	0.459	21.5	$f_1 + f_3 + f_8$
30	24.3602(1)	0.439	8.3	$f_7 - 2f_8$
31	52.2379(9)	0.416	21.6	$2f_2$
32	29.6703(6)	0.403	6.3	$f_3 + f_7 - f_2 - 2f_8$
33	5.3741(4)	0.392	12.6	$f_3 + f_8 - f_2$
34	5.3091(2)	0.391	12.7	$f_3 - f_2$
35	61.2284(1)	0.389	18.5	$2f_3 + f_8 - f_9$
36	29.8002(8)	0.379	8.2	$f_3 + f_7 - f_2$
37	10.1756(1)	0.376	13.6	$f_3 - f_4$
38	48.9605(1)	0.374	17.5	$f_1 + f_3 - f_8$
39	24.4160(2)	0.364	6.8	$f_2 - f_9$
40	78.7607(8)	0.359	31.7	$f_1 + 2f_3 - f_9$
41	38.8497(8)	0.348	17.6	$f_1 + f_4$
42	11.4168(7)	0.335	12.3	$f_5 - f_1$
43	54.1515(2)	0.308	20.4	$f_3 + 2f_7 - f_2 - 2f_8$
44	27.8969(3)	0.299	9.6	$f_1 + 3f_3 + 2f_8 - f_2 - 2f_5$
45	44.6073(3)	0.297	17.7	$f_1 + f_6$
46	57.5470(3)	0.296	16.8	$f_2 + f_3$
47	80.4535(8)	0.293	28.7	$f_1 + 2f_3$
48	62.9211(7)	0.288	13.0	$2f_3 + f_8$
49	13.9535(1)	0.287	7.5	$2f_1 - f_4$
50	9.41278(8)	0.276	10.1	$f_6 - f_1$
51	4.4830(9)	0.275	9.9	$f_3 + f_8 - f_6$
52	90.8987(7)	0.266	32.0	$3f_3 - 2f_9$
53	57.6120(4)	0.262	15.2	$f_2 + f_3 + f_8$
54	61.0984(9)	0.261	12.2	$2f_3 - f_8 - f_9$
55	54.8187(5)	0.258	15.9	$f_2 + f_6 + f_9$
56	58.3731(7)	0.244	16.5	$f_3 + f_6 - f_8$
57	3.6551(2)	0.241	9.9	$f_4 - f_1$
58	5.2443(3)	0.238	7.5	$f_3 - f_2 - f_8$

Table A1
(Continued)

f_i	Frequency (day^{-1})	Amplitude (mmag)	S/N	Comment
59	10.2405(2)	0.236	7.8	$f_3 + f_8 - f_4$
60	55.1330(4)	0.228	13.7	$f_2 + f_5$
61	41.8733(7)	0.219	11.5	$2f_3 - f_1 - 2f_9$
62	52.6805(3)	0.213	10.8	$f_3 + f_4$
63	3.2188(6)	0.212	7.5	$f_7 - f_4$
64	62.7913(6)	0.220	10.0	$2f_3 - f_8$
65	1.7576(5)	0.209	7.4	$f_2 + 2f_8 - f_7$
66	55.6641(9)	0.198	12.5	$2f_1 + 4f_3 + 2f_8 - f_2 - f_4 - 2f_5$
67	42.3981(8)	0.189	9.5	$f_2 + f_4 + 2f_5 - 2f_3 - 2f_8$
68	2.4788(8)	0.183	6.5	$f_3 + f_8 - f_5$
69	7.6695(6)	0.182	7.3	$2f_3 + f_8 - f_2 - f_5$
70	55.8442(7)	0.177	9.9	$f_3 + f_7 - f_8$
71	42.5049(1)	0.176	10.1	$2f_4$
72	57.4821(2)	0.176	8.2	$f_2 + f_3 - f_8$
73	55.8995(1)	0.175	9.8	$f_3 + f_7$
74	6.9567(4)	0.169	6.8	$f_3 - f_7$
75	45.2589(9)	0.167	9.4	$2f_3 - f_1$
76	75.1444(1)	0.128	14.2	$f_1 + f_2 + f_3$
77	78.8256(8)	0.126	11.3	$f_1 + 2f_3 + f_8 - f_9$
78	78.6958(8)	0.123	10.6	$f_1 + 2f_3 - f_8 - f_9$
79	75.2092(7)	0.096	10.8	$f_1 + f_2 + f_3 + f_8$
80	90.9639(1)	0.085	9.8	$3f_3 + f_8 - 2f_9$
81	75.0793(9)	0.075	8.0	$f_1 + f_2 + f_3 - f_8$
82	94.2843(9)	0.069	9.8	$3f_3$
83	94.3493(4)	0.069	9.7	$3f_3 + f_8$
84	90.8339(8)	0.062	7.3	$3f_3 - f_8 - 2f_9$
85	94.2194(9)	0.048	6.9	$3f_3 - f_8$

ORCID iDs

Zhao-Yu Zuo https://orcid.org/0000-0001-6693-586X
Tao-Zhi Yang https://orcid.org/0000-0002-1859-4949

References

Aerts, C. 2021, RvMP, 93, 015001
Aerts, C., Christensen-Dalsgaard, J., & Kurtz, D. W. 2010, Asteroseismology, Astronomy and Astrophysics Library (Dordrecht: Springer)
Balona, L. A. 2014, MNRAS, 437, 1476
Balona, L. A. 2016, MNRAS, 459, 1097
Bedding, T. R., Murphy, S. J., Crawford, C., et al. 2023, ApJL, 946, L10
Bedding, T. R., Murphy, S. J., Hey, D. R., et al. 2020, Natur, 581, 147
Böhm-Vitense, E. 1958, ZAp, 46, 108
Bowman, D. M., Kurtz, D. W., Breger, M., et al. 2016, MNRAS, 460, 1970
Breger, M. 2000, in ASP Conf. Ser. 210, Delta Scuti and Related Stars, ed. M. Breger & M. Montgomery (San Francisco, CA: ASP), 3
Breger, M., & Bischof, K. M. 2002, A&A, 385, 537
Breger, M., & Bregman, J. N. 1975, ApJ, 200, 343
Breger, M., & Kolenberg, K. 2006, A&A, 460, 167
Breger, M., Lenz, P., & Pamyatnykh, A. A. 2009, MNRAS, 396, 291
Breger, M., & Montgomery, M. H. 2014, ApJ, 783, 89
Breger, M., Stich, J., Garrido, R., et al. 1993, A&A, 271, 482
Brown, T. M., Latham, D. W., Everett, M. E., et al. 2011, AJ, 142, 112
Chaplin, W. J., & Miglio, A. 2013, ARA&A, 51, 353
Chen, X., & Li, Y. 2019, ApJ, 872, 156
Chen, X., Li, Y., Lin, G., et al. 2017, ApJ, 834, 146
Drilling, J. S., Landolt, A. U., et al. 2000, in Allen's Astrophysical Quantities, ed. A. N. Cox (Melville, NY: AIP), 381
Dziembowski, W. 1977, AcA, 27, 203
Dziembowski, W., & Krolikowska, M. 1990, AcA, 40, 19
García Hernández, A., Martín-Ruiz, S., Monteiro, M. J. P. F. G., et al. 2015, ApJL, 811, L29
García Hernández, A., Moya, A., Michel, E., et al. 2009, A&A, 506, 79
García Hernández, A., Moya, A., Michel, E., et al. 2013, A&A, 559, A63
García Hernández, A., Suárez, J. C., Moya, A., et al. 2017, MNRAS, 471, L140
Goupil, M.-J., Dupret, M. A., Samadi, R., et al. 2005, JApA, 26, 249
Holdsworth, D. L., Smalley, B., Gillon, M., et al. 2014, MNRAS, 439, 2078
Jurcsik, J., Sódor, Á., Váradi, M., et al. 2005, A&A, 430, 1049
Koch, D. G., Borucki, W. J., Basri, G., et al. 2010, ApJL, 713, L79
Kolenberg, K., Bryson, S., Szabó, R., et al. 2011, MNRAS, 411, 878
Kolenberg, K., Smith, H. A., Gazeas, K. D., et al. 2006, A&A, 459, 577
Kurtz, D. W., Shibahashi, H., Murphy, S. J., et al. 2015, MNRAS, 450, 3015
Lenz, P., & Breger, M. 2005, CoAst, 146, 53
Li, Y., Bedding, T. R., Murphy, S. J., et al. 2022, NatAs, 6, 673
Lovekin, C. C., & Guzik, J. A. 2017, ApJ, 849, 38
McDonald, I., Zijlstra, A. A., & Watson, R. A. 2017, MNRAS, 471, 770
Montgomery, M. H., & Odonoghue, D. 1999, DSSN, 13, 28
Murphy, S. J., Shibahashi, H., & Kurtz, D. W. 2013, MNRAS, 430, 2986
Niemczura, E., Polińska, M., Murphy, S. J., et al. 2017, MNRAS, 470, 2870
Nowakowski, R. M. 2005, AcA, 55, 1
Paxton, B., Bildsten, L., Dotter, A., et al. 2011, ApJS, 192, 3
Paxton, B., Cantiello, M., Arras, P., et al. 2013, ApJS, 208, 4
Paxton, B., Marchant, P., Schwab, J., et al. 2015, ApJS, 220, 15
Paxton, B., Schwab, J., Bauer, E. B., et al. 2018, ApJS, 234, 34
Paxton, B., Smolec, R., Schwab, J., et al. 2019, ApJS, 243, 10
Qian, S.-B., Li, L.-J., He, J.-J., et al. 2018, MNRAS, 475, 478
Ramón-Ballesta, A., García Hernández, A., Suárez, J. C., et al. 2021, MNRAS, 505, 6217
Ricker, G. R., Winn, J. N., Vanderspek, R., et al. 2015, JATIS, 1, 014003
Rodríguez-Martín, J. E., García Hernández, A., Suárez, J. C., et al. 2020, MNRAS, 498, 1700
Shibahashi, H., & Kurtz, D. W. 2012, MNRAS, 422, 738
Stassun, K. G., Oelkers, R. J., Paegert, M., et al. 2019, AJ, 158, 138
Stellingwerf, R. F. 1979, ApJ, 227, 935
Suárez, J. C., García Hernández, A., Moya, A., et al. 2014, A&A, 563, A7
Sun, X.-Y., Zuo, Z.-Y., Yang, T.-Z., et al. 2021, ApJ, 922, 199
Uytterhoeven, K., Moya, A., Grigahcène, A., et al. 2011, A&A, 534, A125
Van Cleve, J. E., & Caldwell, D. A. 2016, Kepler Science Document KSCI-19033-002, id., 1
Xiang, M., Rix, H.-W., Ting, Y.-S., et al. 2022, A&A, 662, A66
Yang, T., Esamdin, A., Song, F., et al. 2018, ApJ, 863, 195
Yang, T.-Z., & Esamdin, A. 2019, ApJ, 879, 59
Yang, T.-Z., Zuo, Z.-Y., Sun, X.-Y., et al. 2022, ApJ, 936, 48
Yu, J., Bedding, T. R., Stello, D., et al. 2020, MNRAS, 493, 1388
Zong, W., Charpinet, S., Vauclair, G., et al. 2016, A&A, 585, A22
Zwintz, K. 2008, ApJ, 673, 1088